Electronic Stability of Magnetic Fe/Co Superlattices with Monatomic Layer Alternation

G. A. Farnan,[1] C. L. Fu,[2] Z. Gai,[1,3] M. Krcmar,[2] A. P. Baddorf,[1] Zhenyu Zhang,[1,4] and J. Shen[1]

[1]*Condensed Matter Sciences Division, Oak Ridge National Laboratory, Oak Ridge, Tennessee 37831, USA*

[2]*Metals & Ceramics Division, Oak Ridge National Laboratory, Oak Ridge, Tennessee 37831, USA*

[3]*Department of Physics, State Key Laboratory for Mesoscopic Physics, Peking University, Beijing 100871, People's Republic of China*

[4]*Department of Physics, The University of Tennessee, Knoxville, Tennessee 37996, USA*

(Received 26 May 2003; published 26 November 2003)

We report a surprising observation that the growth of the $[\mathrm{Fe(1\ ML)/Co(1\ ML)}]_n$ superlattice of $L1_0$ structure on Cu(100) is stable only up to six atomic layers ($n = 3$), which cannot be rationalized by stress arguments. Instead, first-principles calculations reveal a transition from the $L1_0$ to the $B2$ structure due to the effect of dimensionality on the stability of the electronic structure of the superlattice. Whereas the majority-spin electrons are energetically insensitive to the layer thickness, the minority-spin electrons induce the transition at $n = 3$.

DOI: 10.1103/PhysRevLett.91.226106 PACS numbers: 68.55.Jk, 68.55.Nq, 73.21.Cd

In order to realize certain desired properties of materials, one must often grow artificial structures that are inherently unstable in bulk form. Nevertheless, such structures can be stabilized in reduced dimensions if proper kinetic pathways can be devised to reach such configurations. A compelling example is the formation of superlattices with monatomic layer alternation via thin film growth techniques. The corresponding ordered alloys, whether they exist (FePd [1]) or do not exist (including FeAu [2], CoRu [3], AuCu [4], AuNi [5], and FeCu [6]) in their respective bulk phase diagrams, are stable or at least metastable at room temperature once fabricated in reduced dimensions. These nanostructured materials constructed with atomic-scale precision can have intriguing magnetic properties [2,7], which can be exploited in potential technological applications.

A common feature of all of the above known examples of ordered alloys is that smooth layer-by-layer growth lasts at least up to 44 monolayers, or 22 unit cells in the growth direction. Such a structural stability has been achieved even for systems in which at least one of the constituent elements has a large lattice mismatch with the substrate. For example, AuNi monatomic alloys can be grown to more than 40 unit cells on Au(001), despite the existence of a 13% lattice mismatch between fcc Au and fcc Ni. Until now, the microscopic origins for the stability or metastability of this class of artificial low-dimensional structures remain explored.

In this Letter, we report on the observation of an unusual structural instability in the growth of monatomic FeCo superlattices on a Cu(100) substrate in the $L1_0$ ordered alloy structure. Because Fe [8], Co [9], and the $Fe_{50}Co_{50}$ random alloy [10] can each grow up to tens of layers on Cu(100) via a layer-by-layer mode, and the lattice mismatch involved in each case is relatively small ($\sim$1%), we anticipated that the monoatomic FeCo superlattices on Cu(100) should be another favorable system for layer-by-layer growth. To our surprise, we found that monatomic FeCo superlattices in the $L1_0$ phase can be grown only up to three unit cells (6 ML in total), an observation that cannot be rationalized solely based on stress arguments. First-principles calculations within density functional theory reveal the electronic nature of the structural instability of the $[\mathrm{Fe(1\ ML)/Co(1\ ML)}]_n$ superlattices with varying thickness. Whereas the majority-spin electrons are energetically insensitive to the layer thickness, the minority-spin electrons stabilize the $L1_0$ phase for $n \leq 3$, and recover the stable bulklike $B2$ phase for $n > 3$.

The FeCo $L1_0$ system was prepared in an ultrahigh vacuum chamber (base pressure 1×10^{-10} Torr) equipped with growth facilities for laser molecular beam epitaxy (laser MBE) and thermal MBE. The films were ablated by an excimer laser (248 nm, 5 Hz, 30 ns pulse width, $\sim$3 J/cm^2) from Fe and Co targets (4 N purity) mounted on a six-target computer controlled carrousel. The laser MBE technique was employed because it produces more perfect two-dimensional growth of Fe and Co on Cu(100) than thermal MBE [11], which is essential to realize a high quality $L1_0$ alloy structure. Prior to deposition, the Cu(100) single crystal substrate was cleaned by cycles of Ne^+ sputtering and subsequent annealing at 600 °C until clean Auger spectra and sharp low energy electron diffraction (LEED) spots were obtained. The quality of the $L1_0$ structure was investigated by *in situ* reflection high energy electron diffraction (RHEED), scanning tunneling microscopy (STM), and LEED in a layer-by-layer manner, as well as *ex situ* surface x-ray diffraction at Sector 9 of the Advanced Photon Source, Argonne, managed by the CMC-CAT. The magnetic properties were characterized *in situ* by magneto-optical Kerr effect (MOKE).

Both our *in situ* and *ex situ* characterization give conclusive evidence that an $L1_0$ ordered FeCo alloy can only be formed up to 6 ML. Figure 1 shows (a) the RHEED intensity, (b) STM calibrated surface rms roughness, and

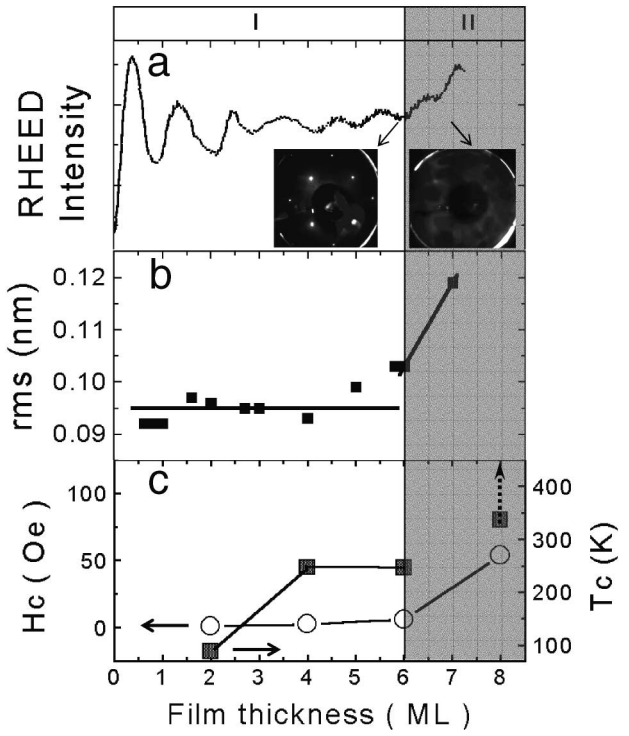

FIG. 1. RHEED intensity (a), STM calibrated surface rms roughness (b), and magnetic coercivity (open circles) and Curie temperature (filled squares) (c) as a function of the Fe/Co film thickness. In growth regime I, films grow layer by layer and, in regime II, significant surface roughening occurs. The inset pictures of (a) are the corresponding LEED patterns (142 eV) of the two growth regimes.

(c) magnetic coercivity (at room temperature) and Curie temperature as a function of the film thickness. All data indicate that the growth of the FeCo monatomic alloy can be divided into two regimes. In regime I (below and up to 6 ML of total thickness), the 1 ML Fe/1 ML Co films grow layer by layer as indicated by the RHEED oscillations [12]. Sharp (1×1) LEED spots were observed for all film thickness within this regime (inset picture). In regime II (beyond 6 ML of total thickness), the LEED could only detect high background without any clearly visible diffraction spots. The films become rougher as evidenced by the gradual disappearance of RHEED oscillations and a sharp increase of the rms roughness. MOKE measurements [Fig. 1(c)] show increased coercivity due to surface roughening above 6 ML. The Curie temperature [Fig. 1(c)], while already levels out at 250 °C for 4 and 6 ML films (regime I), shoots up well beyond 350 °C (maximum measuring temperature) for an 8 ML film (regime II). The definition or division of the two growth regimes does not change if the growth is begun with either Fe or Co showing a minimum effect of the substrate on the structural transition.

Direct evidence that the $L1_0$ structure forms only in regime I is provided by x-ray diffraction. Several films were capped *in situ* with ~50 ML of copper added by MBE, then transported to the Advanced Photon Source. Samples were there mounted inside an evacuated beryllium dome at the center of a six-circle diffractometer on insertion device beam line 9A. This beam line utilizes a cryogenically cooled double-crystal monochromator manufactured by Khozu. Since Fe, Co, and Cu have very little contrast in x-ray scattering, the x-ray energy was set just below the Co edge (7705 eV). At this energy, the scattering contrast is several times greater than away from the edge.

Figure 2 shows the x-ray reflectivity from a sample with three unit cells of FeCo (6 ML total). Data were collected by integrating rocking curves to obtain the full reflectivity for each momentum value. The absolute reflectivity scale was determined by scaling near-Bragg intensities to kinematic calculations. The dominant features are the diffraction from bulk copper at momentum transfer $L = 0, 2$. The next largest feature, at $L = 1.5$, can be identified with the (111) planes of Cu_2O (lattice constant of 4.258 Å) which was formed on the Cu cap during transport of the sample. More interesting for this study is the diffraction intensity near $L = 1$. This peak is clearly associated with the FeCo layers, since it is not observed for x-ray energies away from the Co edge (specifically, at 7500 and 8500 eV). Its location at half the distance of the bulk Cu peak in reciprocal space indicates a doubling of the real space lattice, precisely that expected for an $L1_0$ structure. In addition, the relative intensity of the peak is consistent with kinematic calculations for three unit cells of FeCo, although the absolute intensity is lowered and any intensity oscillations through the Brillouin zone appear to be washed out by the roughness of the Cu-Cu_2O and Cu_2O-vacuum interfaces.

In regime II, the $L1_0$ order is destroyed by the abrupt roughening process above 6 ML. A noticeable feature of the rough films is the lack of distinguishable LEED

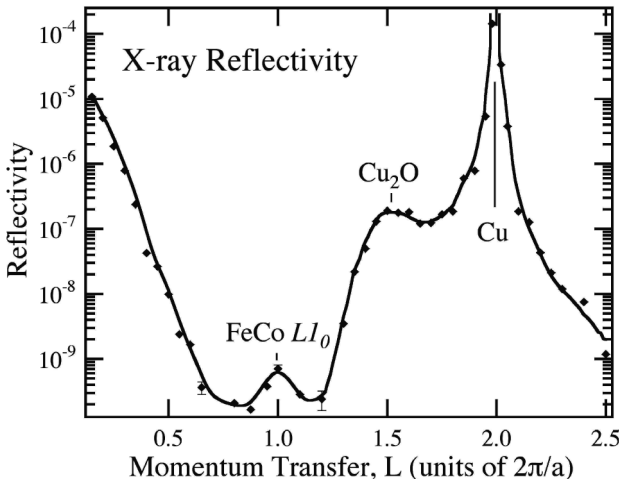

FIG. 2. *Ex situ* x-ray reflectivity from a three bilayer film of FeCo capped with Cu. Diffraction peaks from the Cu substrate, a surface Cu oxide, and the FeCo film are observed. Diffraction intensity and location are consistent with an $L1_0$ structure with little intermixing.

patterns, which is often a sign of either an amorphous phase or a rough surface with nanometer-sized, randomly oriented grains. Figure 3 shows the STM images of films right before (5.5 ML) (a) and after the transition (8 ML) (b). The corresponding histograms (inset) reveal that the films have a regular fcc(100) step height (~0.18 nm) before the transition, but after the transition become rougher with irregular step heights that may reflect structures with various kinds of orientations. For a sample prepared with 10 ML total thickness of FeCo, no x-ray diffraction was observed at $L = 1$, although peaks associated with Cu and Cu_2O were comparable to those in Fig. 2.

To understand the exact cause of this unexpected quick collapse of the FeCo $L1_0$ phase, we have studied the structural stability of both bulk FeCo and (001)-oriented thin Fe/Co slabs using first-principles calculations. We employed the full-potential augmented plane wave method [13] to solve the local-density-functional equation, within the generalized gradient approximation [14] for the exchange-correlation potential. The bulk FeCo with equiatomic composition is stabilized in the bcc-based $B2$ structure by the presence of ferromagnetism with magnetic moments of $1.82\mu_B$ and $2.83\mu_B$ on the Co and Fe sites, respectively. The lattice constant of the $B2$ phase (2.85 Å), however, differs considerably from the in-plane lattice spacing (2.55 Å) of the Cu(001) substrate.

Figure 4 shows the total energy of bulk FeCo in the ordered face-centered-tetragonal (fct) structure as a function of the c/a ratio. Our attention is focused on two particular c/a ratios of the fct structure, i.e., $c/a = 1$ (fcc-based ideal $L1_0$ structure) and 0.71 (bcc-based $B2$ structure). For bulk FeCo, although the total energy is minimized at $c/a = 0.71$, there is a "shoulder" in the energy-versus-c/a curve near $c/a = 1.0$. Such a shoulder indicates that a structural transformation is possible when atoms are in a different environment than in the bulk.

Indeed, our calculations on thin layers of Fe/Co monoatomic superlattices indicate that the shoulder is developed into a true energy minimum in reduced dimensionality. We have calculated the total energies of seven, five, and three atomic layer slabs with both Fe- and Co-terminated surfaces. The surfaces are described by periodic slabs and separated by a seven-layer vacuum. The averaged energy per atom in the slabs as a function of c/a ratio is also shown in Fig. 4, in which the energy of the $B2$ phase is set as a reference in each case (i.e., as zero energy). A truly remarkable effect is found regardless of the type of surface termination: For the seven-layer slabs, a local energy minimum is developed near $c/a = 1.0$ (i.e., in the shoulder region of the bulk energy-versus-c/a curve), however, the slab maintains the absolute energy minimum at the c/a ratio close to that of the bulk $B2$ structure; for the five-layer slabs, the system stabilizes near the $c/a = 1.0$ region, whereas the minimum corresponding to the $B2$ structure begins to disappear; for the three-layer slabs, the slab is stabilized near $c/a = 1.05$–1.10, whereas the structure near $c/a = 0.71$ becomes unstable. Therefore, the effect of the reduced dimensionality is to induce a structural change in the

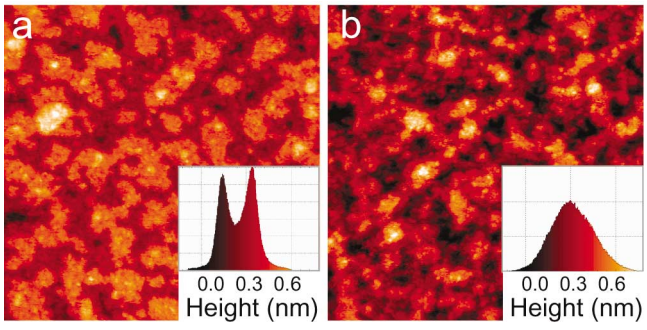

FIG. 3 (color). 50 nm × 50 nm STM images of a 5.5 ML (a) and an 8 ML Fe/Co film (b). The corresponding histograms (inset pictures) indicate that, while the 5.5 ML film has a regular step height of ~0.18 nm, the 8 ML film becomes rougher with irregular step heights.

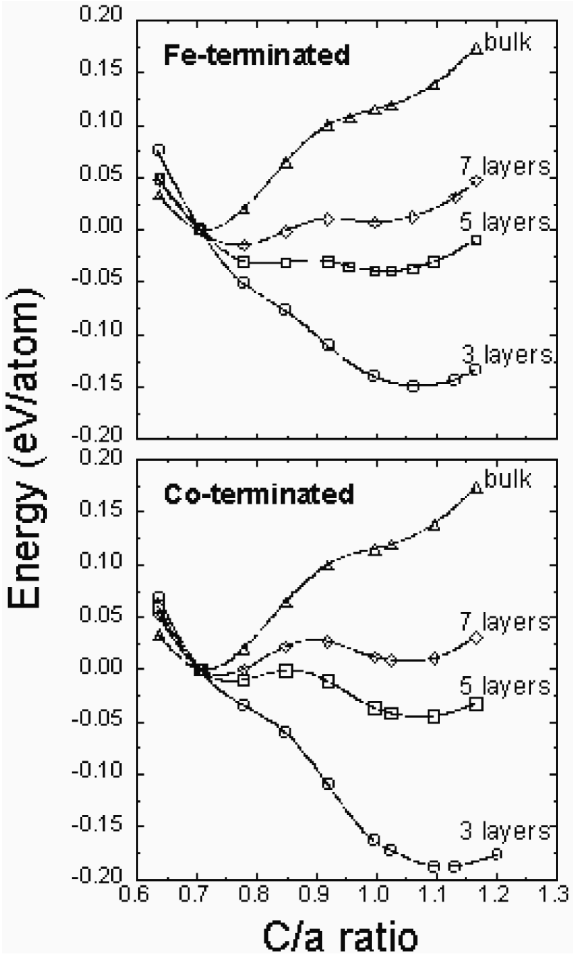

FIG. 4. The total energy of Fe-terminated (top) and Co-terminated (bottom) slabs as a function of c/a ratio. The energy of the $B2$ structure is set as the reference in each case (i.e., as zero energy).

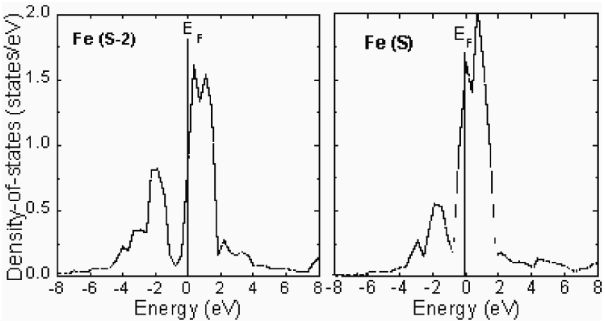

FIG. 5. The layer-projected minority-spin density of states for the Fe-terminated seven-layer slab with $B2$ structure. For comparison, only those of the inner $(S-2)$ (left) and surface (S) (right) Fe layers are shown.

Fe/Co slabs, from the $B2$ structure (for seven or more atomic layers) to the $L1_0$ structure (for five or less atomic layers).

These calculated results provide a clear picture for the experimental observations. At low thickness, the system prefers, energetically, to be in $L1_0$ structure, which has a lattice constant (3.58 Å for $c/a = 1.0$) sufficiently close to that of Cu (3.61 Å) allowing a good layer-by-layer growth. At higher thickness, the system can minimize its energy by transforming into the more stable $B2$ phase. However, because the $B2$ structure has a large lattice mismatch with Cu ($\sim$12%), layer-by-layer growth breaks down and a significant surface roughening is thus observed experimentally. Note that the structural change occurs for the slab thickness between five and seven layers, which agrees well with experimental findings of 6 ML (Fig. 1).

Finally, we discuss the electronic origin of this thickness-driven structural phase transformation. In the Fe/Co slabs, the majority-spin states are nearly fully occupied; therefore, our discussions below are focused on the minority-spin channel, which determines the structural stability of thin Fe/Co slabs. The electronic structure of bulk $B2$ FeCo is characterized by the presence of a pseudogap separating the bonding and nonbonding states. In Fig. 5, we show the layer-projected electron density of states (DOS) of the Fe-terminated seven-layer slab with the $B2$ structure. For the bulklike Fe atoms, the Fermi level (E_F) is located near the valley of the pseudogap; on the other hand, for the surface Fe atoms, the band narrowing smears out the pseudogap in the local DOS profile, resulting in a high DOS at E_F [$N(E_F)$]. The surface atoms therefore exhibit slightly enhanced magnetic moments but have much higher $N(E_F)$ than the bulklike atoms. Therefore, the structural stability of the $B2$ Fe/Co slabs will depend on the surface-to-bulk volume ratio. From our calculations for layer thickness less than or equal to five layers, the $B2$ structure becomes unstable. By contrast, in the close-packed $L1_0$ structure (with $c/a \sim 1$), the separation between the bonding and nonbonding states in the DOS profile is less well-defined than that of the open $B2$ structure, because the electronic interaction in the $L1_0$ structure is no longer dominated by the nearest-neighbor interaction as in the $B2$ structure. An examination on the layer-projected DOS of the seven-layer slab with the $L1_0$ structure shows that, while the band narrowing is still present at the surface, the change of $N(E_F)$ from the center layer to the surface layer is insignificant. In other words, although the bulk FeCo is stabilized in the $B2$ structure, it is far more costly in energy to create a surface on the $B2$ lattice than on the $L1_0$ lattice. As a result, the $L1_0$ structure becomes lower in energy than the $B2$ structure as the number of layers in the slabs decreases. We note that, though the calculation is performed on freestanding Fe/Co slabs, the overall mechanism presented here is expected to be valid even in the presence of the Cu(001) substrate, since the electronic d states of Fe/Co near E_F are hardly affected by Cu due to clear separation between their d bands.

In conclusion, we have observed a surprisingly unstable monoatomically deposited FeCo $L1_0$ structure. This instability is not caused by conventional epitaxial stress in the thin film system. Instead, it is a direct reflection of an $L1_0 \rightarrow B2$ structural phase transition induced by the relative electronic stability of the two alloy phases in reduced dimensionality, as revealed by first-principles calculations.

This work was sponsored by the U.S. Department of Energy, under Contract No. DE-AC05-00-OR22725 with the Oak Ridge National Laboratory, managed by UT-Battelle, LLC.

[1] V. Gehanno *et al.*, J. Magn. Magn. Mater. **172**, 26 (1997).
[2] K. Takanashi *et al.*, Appl. Phys. Lett. **67**, 1016 (1995).
[3] K. Takanashi *et al.*, Surf. Sci. **493**, 713 (2001).
[4] M. Dynna *et al.*, Acta Mater. **45**, 257 (1997).
[5] G. Abadias *et al.*, J. Cryst. Growth **222**, 685 (2001).
[6] S. S. Manoharan *et al.*, Phys. Rev. B **58**, 8549 (1998).
[7] T. Shima *et al.*, Appl. Phys. Lett. **80**, 288 (2002).
[8] H. Jenniches *et al.*, Phys. Rev. B **59**, 1196 (1999); J. Thomassen *et al.*, Phys. Rev. Lett. **69**, 3831 (1992).
[9] J. Fassbender *et al.*, Phys. Rev. Lett. **75**, 4476 (1995).
[10] M. Zharnikov *et al.*, J. Magn. Magn. Mater. **165**, 250 (1997).
[11] H. Jenniches *et al.*, Appl. Phys. Lett. **69**, 3339 (1996).
[12] The maxima of RHEED intensity appearing at half completion of layers indicate that the RHEED geometry was set at close to "in-phase" condition, which gives rise to RHEED oscillations due to diffuse scattering from step edges [e.g., see U. Korte and P. A. Maksym, Phys. Rev. Lett. **78**, 2381 (1997)].
[13] E. Wimmer *et al.*, Phys. Rev. B **24**, 864 (1981).
[14] J. P. Perdew, K. Burke, and M. Ernzerhof, Phys. Rev. Lett. **77**, 3865 (1996).